

Layer-wise Adaptive Gradient Sparsification for Distributed Deep Learning with Convergence Guarantees

Shaohuai Shi, Zhenheng Tang, Qiang Wang, Kaiyong Zhao and Xiaowen Chu

Department of Computer Science, Hong Kong Baptist University
 {csshshi,zhtang,qiangwang,kyzhao,chxw}@comp.hkbu.edu.hk

Abstract

To reduce the long training time of large deep neural network (DNN) models, distributed synchronous stochastic gradient descent (S-SGD) is commonly used on a cluster of workers. However, the speedup brought by multiple workers is limited by the communication overhead. Two approaches, namely pipelining and gradient sparsification, have been separately proposed to alleviate the impact of communication overheads. Yet, the gradient sparsification methods can only initiate the communication after the backpropagation, and hence miss the pipelining opportunity. In this paper, we propose a new distributed optimization method named LAGS-SGD, which combines S-SGD with a novel layer-wise adaptive gradient sparsification (LAGS) scheme. In LAGS-SGD, every worker selects a small set of “significant” gradients from each layer independently whose size can be adaptive to the communication-to-computation ratio of that layer. The layer-wise nature of LAGS-SGD opens the opportunity of overlapping communications with computations, while the adaptive nature of LAGS-SGD makes it flexible to control the communication time. We prove that LAGS-SGD has convergence guarantees and it has the same order of convergence rate as vanilla S-SGD under a weak analytical assumption. Extensive experiments are conducted to verify the analytical assumption and the convergence performance of LAGS-SGD. Experimental results show that LAGS-SGD achieves from around 40% to 95% of the maximum benefit of pipelining on a 16-node GPU cluster. Combining the benefit of pipelining and sparsification, the speedup of LAGS-SGD over S-SGD ranges from $2.86\times$ to $8.52\times$ on our tested CNN and LSTM models, without losing obvious model accuracy.

1 Introduction

With increasing data volumes and model sizes of deep neural networks (DNNs), distributed training is commonly adopted to accelerate the training process among multiple workers. Current distributed stochastic gradient descent (SGD) approaches can be categorized into three types, synchronous (Dekel et al. 2012; Li et al. 2014), asynchronous (Zinkevich et al. 2010) and stall synchronous (Ho et al. 2013). Synchronous SGD (S-SGD) with data-parallelism is the most widely used one in distributed deep learning due to its good convergence properties (Dean et al. 2012; Goyal et al. 2017). However, S-SGD requires iterative syn-

chronization and communication of dense gradient/parameter aggregation among all the workers. Compared to the computing speed of modern accelerators (e.g., GPUs and TPUs), the network speed is usually slow which makes communications a potential system bottleneck. Even worse, the communication time usually grows with the size of the cluster (You, Buluç, and Demmel 2017). Many recent studies focus on alleviating the impact of communications in S-SGD to improve the system scalability. These studies include the system-level methods and the algorithm-level methods.

On the system level, pipelining (Zhang et al. 2017; Goyal et al. 2017; Mori et al. 2017; Li et al. 2018; Shi, Chu, and Li 2019; Harlap et al. 2019) is used to overlap the communications with the computations by exploiting the layer-wise structure of backpropagation during the training process of deep models. On the algorithmic level, researchers have proposed gradient quantization (fewer bits for a number) and sparsification (zero-out gradients that are not necessary to be communicated at the current iteration) techniques for S-SGD to reduce the communication traffic with negligible impact on the model convergence (Alistarh et al. 2017; Chen et al. 2018; Lin et al. 2018; Wen et al. 2017; Wu et al. 2018). The gradient sparsification method is more aggressive than the gradient quantization method in reducing the communication size. For example, Top- k sparsification (Aji and Heafield 2017; Lin et al. 2018) with error compensation can zero-out 99% – 99.9% local gradients without loss of accuracy while quantization from 32-bit floating points to 1-bit has a maximum of $32\times$ size reduction (Wen et al. 2017). In this paper, we mainly focus on the sparsification methods, while our proposed algorithm and analysis are also applicable to the quantization methods.

A number of recent work has investigated the theoretical convergence properties of the gradient sparsification schemes under different analytical assumptions (Wangni et al. 2018; Stich, Cordonnier, and Jaggi 2018; Alistarh et al. 2018; Jiang and Agrawal 2018; Ivkin et al. 2019). However, these gradient sparsification methods ignore the layer-wise structure of DNN models and treat all model parameters as a single vector to derive the convergence bounds, which implicitly requires a single-layer communication (You, Buluç, and Demmel 2017) at the end of each SGD iteration. Therefore,

the current gradient sparsification S-SGD (denoted by SLGS-SGD hereafter) cannot overlap the gradient communications with backpropagation computations, which limits the system scaling efficiency. To tackle this challenge, we propose a new distributed optimization algorithm named LAGS-SGD which exploits a layer-wise adaptive gradient sparsification (LAGS) scheme atop S-SGD to increase the system scalability. We also derive the convergence bounds for LAGS-SGD. Our theoretical convergence results on LAGS-SGD conclude that high compression ratios would slow down the model convergence rate, which indicates that one should choose the compression ratios for different layers as low as possible. The adaptive nature of LAGS-SGD provides flexible options to choose the compression ratios according to the communication-to-computation ratios. We evaluate our proposed algorithm on various DNNs to verify the soundness of the weak analytic assumption and the convergence results. Finally, we demonstrate our system implementation of LAGS-SGD to show the wall-clock training time improvement on a 16-node GPU cluster connected with 1Gbps Ethernet. The contributions of this work are summarized as follows.

- We propose a new distributed optimization algorithm named LAGS-SGD with convergence guarantees. The proposed algorithm enables us to embrace the benefits of both pipelining and gradient sparsification.
- We provide thorough convergence analysis of LAGS-SGD on non-convex smooth optimization problems, and the derived theoretical results indicate that LAGS-SGD has a consistent convergence guarantee with SLGS-SGD, and it has the same order of convergence rate with S-SGD under a weak analytical assumption.
- We empirically verify the analytical assumption and the convergence performance of LAGS-SGD on various deep neural networks including CNNs and LSTM in a distributed setting.
- We implement LAGS-SGD atop PyTorch¹, which is one of the popular deep learning frameworks, and evaluate the training efficiency of LAGS-SGD on a 16-GPU cluster connected with 1Gbps Ethernet. Experimental results show that LAGS-SGD can achieve around 40% to 95% of the maximum benefit of pipelining over state-of-the-art SLGS-SGD. Compared to S-SGD without sparsification, LAGS-SGD can train the model up to $8.52\times$ faster with little impact on the model accuracy.

2 Related Work

Many recent works have provided convergence analysis for distributed SGD with quantified or sparsified gradients that can be biased or unbiased.

For the unbiased quantified or sparsified gradients, researchers (Alistarh et al. 2017; Wen et al. 2017) derived the convergence guarantees for lower-bit quantified gradients, while the quantization operator applied on gradients should be unbiased to guarantee the theoretical results. On the gradient sparsification algorithm whose sparsification method

is also unbiased, Wangni et al. (Wangni et al. 2018) derived the similar theoretical results. However, empirical gradient sparsification methods (e.g., Top- k sparsification (Lin et al. 2018)) can be biased, which require some other analytical techniques to derive the bounds. In this paper, we also mainly focus on the bias sparsification operators like Top- k sparsification.

For the biased quantified or sparsified gradients, Cordonnier (Cordonnier 2018) and Stich et al. (Stich, Cordonnier, and Jaggi 2018) provided the convergence bound for top- k or random- k gradient sparsification algorithms on only convex problems. Jiang et al. (Jiang and Agrawal 2018) derived similar theoretical results, but they exploited another strong assumption that requires each worker to select the same k components at each iteration so that the whole d (the dimension of model/gradient) components are exchanged after a certain number of iterations. Alistarh et al. (Alistarh et al. 2018) relaxed these strong assumptions on sparsified gradients, and further proposed an analytical assumption, in which the ℓ_2 -norm of the difference between the top- k elements on fully aggregated gradients and the aggregated results on locally top- k gradients is bounded. Though the assumption is relaxed, it is difficult to verify in real-world applications. Our convergence analysis is relatively close to the study (Shi et al. 2019) which provided convergence analysis on the biased Top- k sparsification with an easy-to-verify analytical assumption.

The above mentioned studies, however, view all the model parameters (or gradients) as a single vector to derive the convergence bounds, while we propose the layer-wise gradient sparsification algorithm which breaks down full gradients into multiple pieces (i.e., multiple layers). It is obvious that breaking a vector into pieces and selecting top- k elements from each piece generates different results from the top- k elements on the full vector, which makes the proofs of the bounds of LAGS-SGD non-trivial. Recently, (Zheng, Huang, and Kwok 2019) proposed the blockwise SGD for quantified gradients, but it lacks of convergence guarantees for sparsified gradients. Simultaneous to our work, (Dutta et al. 2020) proposed related layer-wise compression schemes.

3 Preliminaries

We consider the common settings of distributed synchronous SGD with data-parallelism on P workers to minimize the non-convex objective function $f : \mathbb{R}^d \rightarrow \mathbb{R}$ by:

$$\mathbf{x}_{t+1} = \mathbf{x}_t - \alpha_t \frac{1}{P} \sum_{p=1}^P G^p(\mathbf{x}_t), \quad (1)$$

where $\mathbf{x}_t \in \mathbb{R}^d$ is the stacked layer-wise model parameters of the target DNN at iteration t , $G^p(\mathbf{x}_t)$ is the stochastic gradients of the DNN parameters at the p^{th} worker with locally sampled data, and $\alpha_t \in \mathbb{R}$ is the step size (i.e., learning rate) at iteration t . Let L denote the number of learnable layers of the DNN, and $\mathbf{x}^{(l)} \in \mathbb{R}^{d^{(l)}}$ denote the parameter vector of the l^{th} learnable layer with $d^{(l)}$ elements². Thus, the model

¹<https://pytorch.org/>

²This generalization is also applicable to the current deep learning frameworks (e.g., PyTorch), in which the parameters of one

parameter \mathbf{x} can be represented by the concatenation of L layer-wise parameters. Using \sqcup as the concatenation operator, the stacked vector can be represented by

$$\mathbf{x} = \sqcup_{l=1}^L \mathbf{x}^{(l)} = \mathbf{x}^{(1)} \sqcup \mathbf{x}^{(2)} \sqcup \dots \sqcup \mathbf{x}^{(L)} = [\mathbf{x}^{(1)}, \mathbf{x}^{(2)}, \dots, \mathbf{x}^{(L)}]. \quad (2)$$

Pipelining between communications and computations. Due to the fact that the gradient computation of layer $l - 1$ using the backpropagation algorithm has no dependency on the gradient aggregation of layer l , the layer-wise communications can then be pipelined with layer-wise computations (Zhang et al. 2017) as shown in Fig. 1(a). It can be seen that some communication time can be overlapped with the computations so that the wall-clock iteration time is reduced. Note that the pipelining technique with full gradients has no side-effect on the convergence, and it becomes very useful when the communication time is comparable to the computing time.

Top- k sparsification. In the gradient sparsification method, the Top- k sparsification with error compensation (Aji and Heafield 2017; Lin et al. 2018) is widely used for distributed training, and its convergence property has been empirically (Aji and Heafield 2017; Lin et al. 2018) verified and theoretically (Alistarh et al. 2018; Jiang and Agrawal 2018; Stich, Cordonnier, and Jaggi 2018) proved under some assumptions. The model update formula of Top- k S-SGD can be represented by

$$\mathbf{x}_{t+1} = \mathbf{x}_t - \alpha_t \frac{1}{P} \sum_{p=1}^P \tilde{G}^p(\mathbf{x}_t), \quad (3)$$

where $\tilde{G}^p(\mathbf{x}_t) = \text{TopK}(G^p(\mathbf{x}_t), k)$ is the selected top- k gradients at worker p . For any vector $\mathbf{x} \in \mathbb{R}^d$ and a given $k \leq d$, $\text{TopK}(\mathbf{x}, k) \in \mathbb{R}^d$ and its i^{th} ($i = 1, 2, \dots, d$) element is:

$$\text{TopK}(\mathbf{x}, k)_i = \begin{cases} x_i, & \text{if } |x_i| > thr \\ 0, & \text{otherwise} \end{cases}, \quad (4)$$

where x_i is the i^{th} element of \mathbf{x} and thr is the k^{th} largest value of $|\mathbf{x}|$. As shown in Fig. 1(b), in each iteration, at the end of the backpropagation pass, each worker selects top- k gradients from its whole set of gradients. The selected k gradients are exchanged with all other workers in the decentralized architecture or sent to the parameter server in the centralized architecture for averaging.

4 Layer-wise Adaptive Gradient Sparsification

Algorithm

To enjoy the benefits of the pipelining technique and the promising gradient sparsification technique, we propose the LAGS-SGD algorithm, which exploits a layer-wise adaptive gradient sparsification (LAGS) scheme atop S-SGD.

In LAGS-SGD, we apply gradient sparsification with error compensation on each layer separately. Instead of selecting the top- k values from all gradients to be communicated, each worker selects top- $k^{(l)}$ gradients from layer l so that it layer may be separated into two tensors (weights and bias).

does not need to wait for the completion of backpropagation pass before communicating the sparsified gradients. LAGS-SGD not only significantly reduces the communication traffic (hence the communication time) using the gradient sparsification, but it also makes use of the layered structure of DNNs to overlap the communications with computations. As shown in Fig. 1(c), at each iteration, after the gradients $G(\mathbf{x})^{(l)}$ of layer l have been calculated, $\text{TopK}(G(\mathbf{x})^{(l)}, k^{(l)})$ is selected to be exchanged among workers immediately.

Formally, let \mathbf{v}_t denote the model parameter and ϵ_t^p denote the local gradient residual of worker p at iteration t . In LAGS-SGD on distributed P workers, the update formula of the layer-wise parameters becomes

$$\mathbf{v}_{t+1}^{(l)} = \mathbf{v}_t^{(l)} - \frac{1}{P} \sum_{p=1}^P \text{TopK} \left(\alpha_t G^p(\mathbf{v}_t)^{(l)} + \epsilon_t^{p,(l)}, k^{(l)} \right), \quad (5)$$

for $l = 1, 2, \dots, L$. The pseudo-code of LAGS-SGD is shown in Algorithm 1.

Algorithm 1 LAGS-SGD at worker p

Input: Stochastic gradients $G^p(\cdot)$ at worker p

Input: Configured layer-wise number of gradients: $k^{(l)}, l = 1, 2, \dots, L$

Input: Configured learning rates α_t

```

1: for  $t = 1 \rightarrow L$  do
2:   Initialize  $\mathbf{v}_0^{(l)} = \epsilon_0^{p,(l)} = 0$ ;
3: end for
4: for  $t = 1 \rightarrow T$  do
5:   Feed-forward computation;
6:   for  $l = L \rightarrow 1$  do
7:      $acc_t^{p,(l)} = \epsilon_{t-1}^{p,(l)} + \alpha_{t-1} G^p(\mathbf{v}_{t-1})^{(l)}$ ;
8:      $\epsilon_t^{p,(l)} = acc_t^{p,(l)} - \text{TopK}(acc_t^{p,(l)}, k^{(l)})$ ;
9:      $\mathbf{g}_t^{(l)} = \sum_{p=1}^P \text{TopK}(acc_t^{p,(l)}, k^{(l)})$ ;
10:     $\mathbf{v}_t^{(l)} = \mathbf{v}_{t-1}^{(l)} - \frac{1}{P} \mathbf{g}_t^{(l)}$ ;
11:   end for
12: end for

```

Convergence Analysis

We first introduce some notations and assumptions for our convergence analysis, and then present the theoretical results of the convergence properties of LAGS-SGD.

Notations and Assumptions. Let $\|\cdot\|$ denote ℓ_2 -norm. We mainly discuss the non-convex objective function $f : \mathbb{R}^d \rightarrow \mathbb{R}$ which has a Lipschitz continuity of C , i.e.,

$$\|\nabla f(\mathbf{x}) - \nabla f(\mathbf{y})\| \leq C \|\mathbf{x} - \mathbf{y}\|, \forall \mathbf{x}, \mathbf{y} \in \mathbb{R}^d. \quad (6)$$

Let \mathbf{x}^* denote the optimal solution of the objective function f . We assume that the sampled stochastic gradients $G(\cdot)$ are unbiased, i.e., $\mathbb{E}[G(\mathbf{v}_t)] = \nabla f(\mathbf{v}_t)$. We also assume that the second moment of the average of P stochastic gradients has the following bound:

$$\mathbb{E} \left\| \frac{1}{P} \sum_{p=1}^P G^p(\mathbf{x}) \right\|^2 \leq M^2, \forall \mathbf{x} \in \mathbb{R}^d. \quad (7)$$

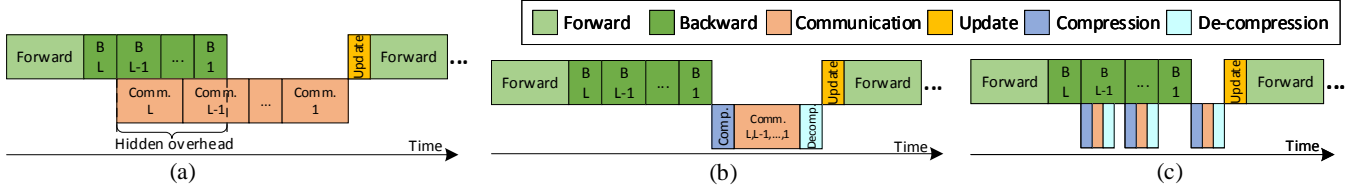


Figure 1: Comparison between three distributed training algorithms: (a) the pipeline of layer-wise gradient communications and backpropagation computations without gradient sparsification (Dense-SGD), (b) the single-layer gradient sparsification (SLGS) without pipelining, and (c) our proposed layer-wise adaptive gradient sparsification (LAGS) with pipelining.

We make an analytical assumption on the aggregated results from the distributed sparsified vectors.

Assumption 1. For any P vectors $\mathbf{x}^p \in \mathbb{R}^d$ ($p = 1, 2, \dots, P$) in P workers, and each vector is sparsified as $\text{TopK}(\mathbf{x}^p, k)$ locally. The aggregation of $\text{TopK}(\mathbf{x}^p, k)$ selects k larger values than randomly selecting k values from the accumulated vectors, i.e.,

$$\left\| \sum_{p=1}^P \mathbf{x}^p - \sum_{p=1}^P \text{TopK}(\mathbf{x}^p, k) \right\|^2 \leq \mathbb{E} \left[\left\| \sum_{p=1}^P \mathbf{x}^p - \text{RandK} \left(\sum_{p=1}^P \mathbf{x}^p, k \right) \right\|^2 \right], \quad (8)$$

where $\text{RandK}(\mathbf{x}, k) \in \mathbb{R}^d$ is a vector whose k elements are randomly selected from \mathbf{x} following a uniform distribution, and the other $d - k$ elements are zeros.

Similar to (Alistarh et al. 2018; Shi et al. 2019), we introduce an auxiliary random variable $\mathbf{x}_t \in \mathbb{R}^d$, which is updated by the non-sparsified gradients, i.e.,

$$\mathbf{x}_{t+1} = \mathbf{x}_t - \alpha_t G(\mathbf{v}_t), \quad (9)$$

where $G(\mathbf{v}_t) = \frac{1}{P} \sum_{p=1}^P G^p(\mathbf{v}_t)$ and $\mathbf{x}_0 = \mathbf{0}$. The error between \mathbf{x}_t and \mathbf{v}_t can be represented by

$$\boldsymbol{\epsilon}_t = \mathbf{v}_t - \mathbf{x}_t = \frac{1}{P} \sum_{p=1}^P \boldsymbol{\epsilon}_t^p. \quad (10)$$

Main Results. Here we present the major lemmas and theorems to prove the convergence of LAGS-SGD, and some proof details are deferred to the supplementary material. Our results are mainly the derivation of the standard bounds in non-convex settings (Bottou, Curtis, and Nocedal 2018), i.e.,

$$\lim_{T \rightarrow \infty} \frac{1}{\sum_{t=1}^T \alpha_t} \sum_{t=1}^T \alpha_t \mathbb{E}[\|\nabla f(\mathbf{v}_t)\|^2] = 0, \quad \text{and } \mathbb{E}[\frac{1}{T} \sum_{t=1}^T \|\nabla f(\mathbf{v}_t)\|^2] \leq B, \quad (11)$$

for some constants B and the number of iterations T .

Lemma 1. For any P vectors $\mathbf{x}^p \in \mathbb{R}^d$, $p = 1, 2, \dots, P$, and every vector can be broken down into L pieces, that is

$\mathbf{x}^p = \sqcup_{l=1}^L \mathbf{x}^{p,(l)}$ and $\mathbf{x}^{p,(l)} \in \mathbb{R}^{d^{(l)}}$, it holds that

$$\left\| \sum_{p=1}^P \mathbf{x}^p - \sqcup_{l=1}^L \left(\sum_{p=1}^P \text{TopK}(\mathbf{x}^{p,(l)}, k^{(l)}) \right) \right\|^2 \leq \left(1 - \frac{1}{c_{max}}\right) \left\| \sum_{p=1}^P \mathbf{x}^p \right\|^2, \quad (12)$$

where $c_{max} = \max\{c^{(1)}, c^{(2)}, \dots, c^{(L)}\}$, $c^{(l)} = \frac{d^{(l)}}{k^{(l)}}$ for $l = 1, 2, \dots, L$, $0 < k^{(l)} \leq d^{(l)}$ and $\sum_{l=1}^L d^{(l)} = d$.

Proof. First we use the fact that has been proved in (Stich, Cordonnier, and Jaggi 2018) in the bound of the RandK operator, i.e., for any vectors $\mathbf{x} \in \mathbb{R}^d$ and $0 < k \leq d$, we have

$$\begin{aligned} & \mathbb{E}_{\omega}[\|\mathbf{x} - \text{RandK}(\mathbf{x}, k)\|^2] \\ &= \frac{1}{|\Omega_k|} \sum_{\omega \in \Omega_k} \sum_{i=1}^d x_i^2 \mathbb{I}\{i \notin \omega\} = \left(1 - \frac{k}{d}\right) \|\mathbf{x}\|^2. \end{aligned}$$

Then under Assumption 1, we obtain

$$\begin{aligned} & \left\| \sum_{p=1}^P \mathbf{x}^p - \sqcup_{l=1}^L \left(\sum_{p=1}^P \text{TopK}(\mathbf{x}^{p,(l)}, k^{(l)}) \right) \right\|^2 \\ &= \left\| \sqcup_{l=1}^L \left(\sum_{p=1}^P \mathbf{x}^{p,(l)} - \sum_{p=1}^P \text{TopK}(\mathbf{x}^{p,(l)}, k^{(l)}) \right) \right\|^2 \\ &= \sum_{l=1}^L \left\| \sum_{p=1}^P \mathbf{x}^{p,(l)} - \sum_{p=1}^P \text{TopK}(\mathbf{x}^{p,(l)}, k^{(l)}) \right\|^2 \\ &\leq \sum_{l=1}^L \mathbb{E} \left[\left\| \sum_{p=1}^P \mathbf{x}^{p,(l)} - \text{RandK} \left(\sum_{p=1}^P \mathbf{x}^{p,(l)}, k^{(l)} \right) \right\|^2 \right] \\ &= \sum_{l=1}^L \left(1 - \frac{k^{(l)}}{d^{(l)}}\right) \left\| \sum_{p=1}^P \mathbf{x}^{p,(l)} \right\|^2 \\ &\leq \left(1 - \frac{1}{c_{max}}\right) \sum_{l=1}^L \left\| \sum_{p=1}^P \mathbf{x}^{p,(l)} \right\|^2 = \left(1 - \frac{1}{c_{max}}\right) \left\| \sum_{p=1}^P \mathbf{x}^p \right\|^2. \end{aligned}$$

□

The inequality (12) is a sufficient condition to derive the convergence properties of Algorithm 1. Proof details of the following corollaries and theorem are provided in the supplementary material.

Corollary 1. For any iteration $t \geq 1$ and $\eta > 0$:

$$\mathbb{E}[\|\mathbf{v}_t - \mathbf{x}_t\|^2] \leq \frac{1}{\eta} \sum_{i=1}^t \left(\left(1 - \frac{1}{c_{max}}\right) (1 + \eta) \right)^i \alpha_{t-i}^2 M^2. \quad (13)$$

Corollary 1 implies that the parameters with sparsified layer-wise gradients have bounds compared to the parameters with dense gradients.

Theorem 1. Under the assumptions defined in the objective function f , after running T iterations with Algorithm 1, we have

$$\begin{aligned} & \frac{1}{\sum_{t=1}^T \alpha_t} \sum_{t=1}^T \alpha_t \mathbb{E}[\|\nabla f(\mathbf{v}_t)\|^2] \\ & \leq \frac{4(f(\mathbf{x}_0) - f(\mathbf{x}^*))}{\sum_{t=1}^T \alpha_t} + \frac{2(C + \frac{2C^2D}{\eta})M^2 \sum_{t=1}^T \alpha_t^2}{\sum_{t=1}^T \alpha_t}, \end{aligned} \quad (14)$$

if one chooses a step size schedule such that $\exists D > 0$ and $\exists \eta > 0$,

$$\sum_{i=1}^t \left(\left(1 - \frac{1}{c_{max}}\right) (1 + \eta) \right)^i \frac{\alpha_{t-i}^2}{\alpha_t} \leq D \quad (15)$$

holds at any iteration $t > 0$.

Theorem 1 indicates that if one chooses the step sizes to satisfy inequality (15), then the right hand side of (14) converges as $T \rightarrow \infty$, so that Algorithm 1 is guaranteed to converge. If we let $(1 - \frac{1}{c_{max}})(1 + \eta) < 1$ which is easily satisfied then inequality (15) holds for constant step sizes and diminishing step sizes. Therefore, if the step sizes are further configured as

$$\lim_{T \rightarrow \infty} \sum_{t=1}^T \alpha_t = \infty \text{ and } \lim_{T \rightarrow \infty} \sum_{t=1}^T \alpha_t^2 < \infty, \quad (16)$$

then the right hand side of inequality (14) converges to zero, which ensures the convergence of Algorithm 1.

Corollary 2. Under the same assumptions in Theorem 1, if $\alpha_t = \theta/\sqrt{T}, \forall t > 0$, where $\theta > 0$ is a constant, then we have the convergence rate bound for Algorithm 1 as:

$$\begin{aligned} \mathbb{E}\left[\frac{1}{T} \sum_{t=1}^T \|\nabla f(\mathbf{v}_t)\|^2\right] & \leq \frac{4\theta^{-1}(f(\mathbf{x}_0) - f(\mathbf{x}^*)) + 2\theta CM^2}{\sqrt{T}} \\ & + \frac{4C^2M^2(c_{max}^3 - c_{max})\theta^2}{T}, \end{aligned} \quad (17)$$

if the total number of iterations T is large enough.

In Corollary 2, if T is large enough, then the right hand side of Eq. (17) is dominated by the first term. It implies that Algorithm 1 has a convergence rate of $O(1/\sqrt{T})$, which is the same as the vanilla SGD (Dekel et al. 2012). However, the

second term of Eq. (17) also indicates that higher compression ratios (i.e., c_{max}) lead to a larger bound of the convergence rate. In real-world settings, one may have a fixed number of iteration budget T to train the model, so high compression ratios could slowdown the convergence speed. On the one hand, if we choose lower compression ratios, then the algorithm has a faster convergence rate (less number of iterations). On the other hand, lower compression ratios have a larger communication size and thus may result in longer wall-clock time per iteration. Therefore, the adaptive selection of the compression ratios tackles the problem properly.

5 System Implementation and Optimization

The layer-wise sparsification nature of LAGS-SGD enables the pipelining technique to hide the communication overheads, while the efficient system implementation of communication and computation parallelism with gradient sparsification is non-trivial due to three reasons: 1) Layer-wise communications with sparsified gradients indicate that there exist many small size messages to be communicated across the network, while collectives (e.g., AllReduce) with small messages are latency-sensitive. 2) Gradient sparsification (especially top- k selection on GPUs) would introduce extra computation time. 3) The convergence rate of LAGS-SGD is negatively effected by the compression ratio, and one should decide proper compression ratios to trade-off the number of iteration to converge and the iteration wall-clock time.

First, we exploit a heuristic method to merge extremely small sparsified tensors to a single one for efficient communication to address the first problem. Specifically, we use a memory buffer to temporarily store the sparsified gradients, and aggregate the buffered gradients once the buffer becomes full or the gradients of the first layer have been calculated. Second, we implement the double sampling method (Lin et al. 2018) to approximately select the top- k gradients, which can significantly reduce the top- k selection time on GPUs. Finally, to achieve a balance between the convergence rate and the training wall-clock time, we propose to select the layer-wise compression ratio according to the communication-to-computation ratio. To be specific, we select a compression ratio $c^{(l)} = d^{(l)}/k^{(l)}$ for layer l such that its communication overhead is appropriately hidden by the computation. Given an upper bound of the compression ratio (e.g., $c_u = 1000$), the algorithm determines $c^{(l)}$ according to the following three metrics: 1) Backpropagation computation time of the pipelined layers (i.e., $t_{comp}^{(l-1)}$); 2) Communication time of the current layer $t_{comm}^{(l)}$ under a specific compression ratio $c^{(l)}$, which can be predicted using the communication model of the AllGather or AllReduce collectives (e.g., (Li et al. 2018; Renggli et al. 2018)) according to the size of gradients and the inter-connection (e.g., latency and bandwidth) between workers; 3) Extra overhead involved by the sparsification operator ($t_{spar}^{(l)}$), which generally includes a pair of operations (compression and de-compression). Therefore, the selected value of $c^{(l)}$ can be generalized as

$$c^{(l)} = \max\{c_u, \min\{c|t_{comm}^{(l)}(c) + t_{spar}^{(l)} \leq t_{comp}^{(l-1)}\}\}. \quad (18)$$

Bound of Pipelining Speedup

In LAGS-SGD, the sparsification technique is used to reduce the overall communication time, and the pipelining technique is used to further overlap the already reduced communication time with computation time. With efficient system implementation of LAGS-SGD, we can analyze the optimal speedup of LAGS-SGD over SLGS-SGD in terms of wall-clock time under the same compression ratios. Let t_f , t_b and t_c denote the forward computation, backward computation and gradient communication time at each iteration respectively. We assume that the sparsification overhead can be ignored as we use the efficient sampling method. Compared to SLGS-SGD, LAGS-SGD reduces the wall-clock time by pipelining the communications with computations, and the maximum overlapped time is $t_{hidden} = \min\{t_b, t_c\}$ (i.e., either backpropagation computations or communications are completely overlapped). So the maximum speedup of LAGS-SGD over SLGS-SGD can be calculated as $S = (t_f + t_b + t_c) / (t_f + t_b + t_c - t_{hidden})$. Let $r = t_c / t_b$ denote the communication-to-computation ratio. The ideal speedup can be represented by

$$S_{max} = 1 + \frac{1}{\frac{t_f}{\min(t_c, t_b)} + \max(r, 1/r)}. \quad (19)$$

The equation shows that the maximum speedup of LAGS-SGD over SLGS-SGD mainly depends on the communication-to-computation ratio (and hence the compression ratios), and is bounded by $1 + t_b / (t_f + t_b)$. If r is close to 1, then LAGS-SGD has the potential to achieve the highest speedup by completely hiding either the backpropagation computation or the communication time.

6 Experiments

Experimental Settings

We conduct the similar experiments as the work (Lin et al. 2018), which cover two types of applications with three data sets: 1) image classification by convolutional neural networks (CNNs) such as ResNet-20 (He et al. 2016) and VGG-16 (Simonyan and Zisserman 2014) on the Cifar-10³ data set and Inception-v4 (Szegedy et al. 2017) and ResNet-50 (He et al. 2016) on the ImageNet (Deng et al. 2009) data set; 2) language model by a 2-layer LSTM model (LSTM-PTB) with 1500 hidden units per layer on the PTB (Marcus, Marcinkiewicz, and Santorini 1993) data set. The the evaluated models, the hyper-parameters are set as follows. On Cifar-10, the mini-batch size for each worker is 32, and the base learning rate is 0.1; On ImageNet, the mini-batch size for each worker is also 32, and the learning rate is 0.01; On PTB, the mini-batch size and learning rate is 20 and 22 respectively. We set the compression ratios as 1, 000 and 250 for CNNs and LSTM respectively. In all compared algorithms, the hyper-parameters are kept the same and experiments are conducted on a distributed 16-GPU environment.

³<http://www.cs.toronto.edu/kriz/cifar.html>

Verification of Assumption 1 and Convergences

To show the soundness of Assumption 1 and the convergence results, we conduct the experiments with 16 workers to train the models. We define metrics $\delta^{(l)}$ ($l = 1, 2, \dots, L$) for each learnable layer during the training process at each iteration with Algorithm 1, and

$$\delta^{(l)} = \frac{\left\| \sum_{p=1}^P \mathbf{x}^{p,(l)} - \sum_{p=1}^P \text{TopK}(\mathbf{x}^{p,(l)}, k^{(l)}) \right\|^2}{\left\| \sum_{p=1}^P \mathbf{x}^{p,(l)} - \text{RandK} \left(\sum_{p=1}^P \mathbf{x}^{p,(l)}, k^{(l)} \right) \right\|^2}, \quad (20)$$

where $\mathbf{x}^{p,(l)} = G^p(\mathbf{v}_t^{(l)}) + \epsilon_t^{p,(l)}$. Assumption 1 holds if $\delta^{(l)} \leq 1$ ($l = 1, 2, \dots, L$). We measure $\delta^{(l)}$ on ResNet-20, VGG-16 and LSTM-PTB during training, and the results are shown in Fig. 2. It is seen that $\delta^{(l)} < 1$ throughout the training process, which implies that Assumption 1 holds. The evaluated models all converge in a certain number of epochs, which verifies the convergence bound of LAGS-SGD.

Comparison of Convergence Rates

In this subsection we compare the validation accuracy of LAGS-SGD with Dense-SGD and SLGS-SGD under the same number of training epochs. The convergence comparison is shown in Fig. 3. The top-1 validation accuracy (the higher the better) on CNNs and the validation perplexity (the lower the better) on LSTM show that LAGS-SGD has very close convergence performance to SLGS-SGD. Compared to Dense-SGD, SLGS-SGD and LAGS-SGD both have slight accuracy losses. The problem could be resolved by some training tricks like warm-up and momentum correction methods (Lin et al. 2018). The final evaluation results are shown in Table 1. The nearly consistent convergence performance between LAGS-SGD and Dense-SGD verify our theoretical results on the convergence rate.

Table 1: Comparison of evaluation performance. Top-1 validation accuracy for CNNs and perplexity for LSTM-PTB.

Model	Dense-SGD	SLGS-SGD	LAGS-SGD
ResNet-20	0.9092	0.8985	0.9024
VGG-16	0.9278	0.9255	0.9227
ResNet-50	0.7191	0.7211	0.7183
LSTM-PTB	106.7	105.7	109.4

Wall-clock Time Performance and Discussions

To illustrate the performance gain of our LAGS-SGD over SLGS-SGD, we evaluate the average iteration time on ResNet-50 and Inception-v4 on ImageNet, and LSTM-PTB on PTB on the 16-GPU cluster connected with 1 Gbps Ethernet. Each node contains an Intel CPU (Celeron N3350) and an Nvidia GPU (P102-100) with Ubuntu-16.04 and CUDA-9.0. The main libraries used in our experiments are PyTorch-v0.4, OpenMPI-3.1.1⁴, Horovod-v0.14⁵ and NCCL-v2.1.15⁶. The

⁴<https://www.open-mpi.org>

⁵<https://github.com/horovod/horovod>

⁶<https://developer.nvidia.com/nccl>

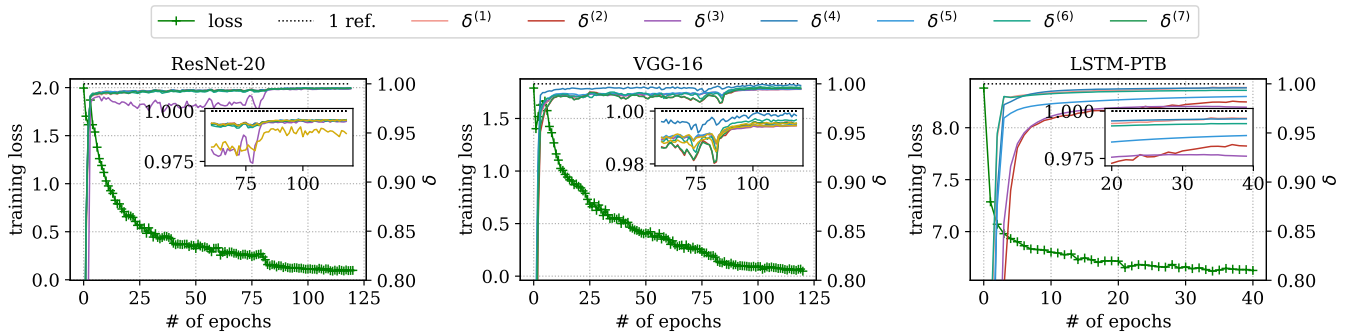


Figure 2: The values of $\delta^{(l)}$ (7 layers are displayed for better visualization), and the training loss of LAGS-SGD on 16 workers.

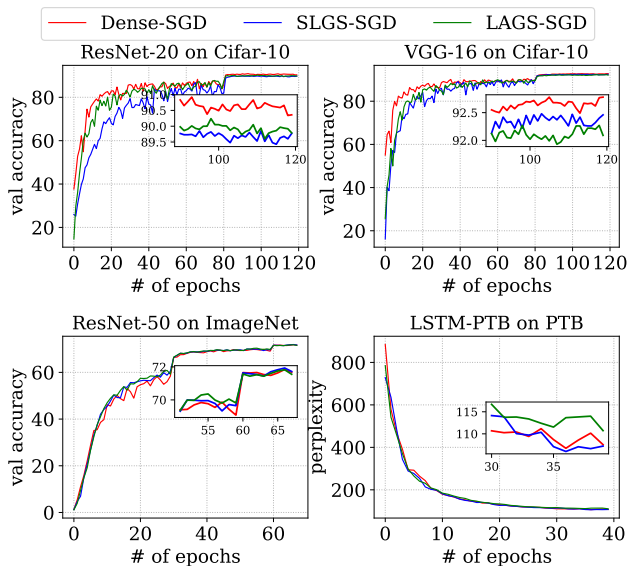


Figure 3: The comparison of convergence performance. Top-1 validation accuracy for CNNs and perplexity for LSTM-PTB.

experimental results are shown in Table 2, which demonstrate that LAGS-SGD performs around 30% faster than SLGS-SGD on ResNet-50 and Inception-v4, while it achieves 11% improvement over SLGS-SGD on LSTM-PTB. The maximum possible speedup of pipelining over SLGS-SGD is calculated by Eq. 19 and shown as S_{max} in Table 2. Our LAGS-SGD achieves 59.6%, 96.5% and 39.3% of S_{max} on ResNet-50, Inception-v4 and LSTM-PTB respectively.

We notice that the achieved speedup of LAGS-SGD over SLGS-SGD on the LSTM-PTB model is relatively small compared to the optimum. The main reason is the unbalanced layer-wise computations and communications. In the real applications, the achievable speedup also depends on the opportunity of the overlap between communications and computations. For example, if a model whose last layer is computation-intensive, while its first layer is communication-intensive, then the speedup of pipelining is marginal as the computation of last layer and the communication of first layer cannot be overlapped as shown in Fig. 1(c). On the

other hand, the achieved improvements of LAGS-SGD over SLGS-SGD on ResNet-50 and Inception-v4 models are very close to the maximum speedups as the communications and computations are both dominated by convolution layers. Furthermore, compared to Dense-SGD, LAGS-SGD runs from $2.86\times$ to $8.52\times$ improved training speeds on the evaluated models.

The layer-wise nature of LAGS-SGD also enables the possibility of scheduling between communications and computations to improve the scalability (Shi, Chu, and Li 2019; Wang, Pi, and Zhou 2019). We leave this as our future work.

Table 2: Comparison of the average iteration wall-clock time (in seconds) of 1000 running iterations. S_1 and S_2 indicate the speedups of LAGS-SGD over Dense-SGD and SLGS-SGD respectively. S_{max} is the maximum speedup of pipelining over SLGS-SGD.

Model	Dense	SLGS	LAGS	S_1	S_2	S_{max}
ResNet-50	1.45s	0.67s	0.51s	2.86	1.31	1.52
Inception-v4	3.85s	1.60s	1.25s	3.08	1.28	1.29
LSTM-PTB	7.80s	1.02s	0.92s	8.52	1.11	1.28

7 Conclusion

In this paper, we proposed a new distributed optimization algorithm for deep learning named LAGS-SGD, which exploits a novel layer-wise adaptive gradient sparsification scheme to embrace the promising pipelining techniques and gradient sparsification methods. LAGS-SGD not only takes advantage of the gradient sparsification algorithm to reduce the communication size, but also makes use of the pipelining technique to further hide the communication overhead. We provided detailed theoretical analysis for LAGS-SGD which showed that LAGS-SGD has convergence guarantees and the consistent convergence rate as the original Dense-SGD under a weak analytical assumption. We ran extensive experiments to verify the soundness of the analytical assumption and theoretical results. Experimental results on a 16-node GPU cluster connected with 1Gbps Ethernet network demonstrated that LAGS-SGD achieves much faster training speed (the wall-clock time) than the state-of-the-art sparsified S-SGD and Dense-SGD with comparable model accuracy.

References

- [Aji and Heafield 2017] Aji, A. F., and Heafield, K. 2017. Sparse communication for distributed gradient descent. In *Proceedings of the 2017 Conference on Empirical Methods in Natural Language Processing*, 440–445.
- [Alistarh et al. 2017] Alistarh, D.; Grubic, D.; Li, J.; Tomioka, R.; and Vojnovic, M. 2017. QSGD: Communication-efficient SGD via gradient quantization and encoding. In *Advances in Neural Information Processing Systems*, 1709–1720.
- [Alistarh et al. 2018] Alistarh, D.; Hoefler, T.; Johansson, M.; Konstantinov, N.; Khirirat, S.; and Renggli, C. 2018. The convergence of sparsified gradient methods. In *Advances in Neural Information Processing Systems*, 5977–5987.
- [Bottou, Curtis, and Nocedal 2018] Bottou, L.; Curtis, F. E.; and Nocedal, J. 2018. Optimization methods for large-scale machine learning. *Siam Review* 60(2):223–311.
- [Chen et al. 2018] Chen, C.-Y.; Choi, J.; Brand, D.; Agrawal, A.; Zhang, W.; and Gopalakrishnan, K. 2018. AdaComp: Adaptive residual gradient compression for data-parallel distributed training. In *Proceedings of the Thirty-Second AAAI Conference on Artificial Intelligence*.
- [Cordonnier 2018] Cordonnier, J.-B. 2018. Convex optimization using sparsified stochastic gradient descent with memory. Technical report.
- [Dean et al. 2012] Dean, J.; Corrado, G.; Monga, R.; Chen, K.; Devin, M.; Mao, M.; Senior, A.; Tucker, P.; Yang, K.; Le, Q. V.; et al. 2012. Large scale distributed deep networks. In *Advances in neural information processing systems*, 1223–1231.
- [Dekel et al. 2012] Dekel, O.; Gilad-Bachrach, R.; Shamir, O.; and Xiao, L. 2012. Optimal distributed online prediction using mini-batches. *Journal of Machine Learning Research* 13(Jan):165–202.
- [Deng et al. 2009] Deng, J.; Dong, W.; Socher, R.; Li, L.-J.; Li, K.; and Fei-Fei, L. 2009. ImageNet: A large-scale hierarchical image database. In *Computer Vision and Pattern Recognition, 2009. CVPR 2009. IEEE Conference on*, 248–255. IEEE.
- [Dutta et al. 2020] Dutta, A.; Bergou, E. H.; Abdelmoniem, A. M.; Ho, C.-Y.; Sahu, A. N.; Canini, M.; and Kalnis, P. 2020. On the discrepancy between the theoretical analysis and practical implementations of compressed communication for distributed deep learning. In *Proc. of AAAI*.
- [Goyal et al. 2017] Goyal, P.; Dollár, P.; Girshick, R.; Noordhuis, P.; Wesolowski, L.; Kyrola, A.; Tulloch, A.; Jia, Y.; and He, K. 2017. Accurate, large minibatch SGD: Training ImageNet in 1 hour. *arXiv preprint arXiv:1706.02677*.
- [Harlap et al. 2019] Harlap, A.; Narayanan, D.; Phanishayee, A.; Seshadri, V.; Devanur, N.; Ganger, G.; and Gibbons, P. 2019. PipeDream: Fast and efficient pipeline parallel DNN training. *Proceedings of the 2nd SysML Conference*.
- [He et al. 2016] He, K.; Zhang, X.; Ren, S.; and Sun, J. 2016. Deep residual learning for image recognition. In *Proceedings of the IEEE conference on computer vision and pattern recognition*, 770–778.
- [Ho et al. 2013] Ho, Q.; Cipar, J.; Cui, H.; Lee, S.; Kim, J. K.; Gibbons, P. B.; Gibson, G. A.; Ganger, G.; and Xing, E. P. 2013. More effective distributed ML via a stale synchronous parallel parameter server. In *Advances in neural information processing systems*, 1223–1231.
- [Ivkin et al. 2019] Ivkin, N.; Rothchild, D.; Ullah, E.; Braverman, V.; Stoica, I.; and Arora, R. 2019. Communication-efficient distributed sgd with sketching. *arXiv preprint arXiv:1903.04488*.
- [Jiang and Agrawal 2018] Jiang, P., and Agrawal, G. 2018. A linear speedup analysis of distributed deep learning with sparse and quantized communication. In *Advances in Neural Information Processing Systems*, 2530–2541.
- [Li et al. 2014] Li, M.; Zhang, T.; Chen, Y.; and Smola, A. J. 2014. Efficient mini-batch training for stochastic optimization. In *Proceedings of the 20th ACM SIGKDD international conference on Knowledge discovery and data mining*, 661–670. ACM.
- [Li et al. 2018] Li, Y.; Yu, M.; Li, S.; Avestimehr, S.; Kim, N. S.; and Schwing, A. 2018. Pipe-SGD: A decentralized pipelined SGD framework for distributed deep net training. In *Advances in Neural Information Processing Systems*, 8045–8056.
- [Lin et al. 2018] Lin, Y.; Han, S.; Mao, H.; Wang, Y.; and Dally, W. J. 2018. Deep gradient compression: Reducing the communication bandwidth for distributed training. In *International Conference on Learning Representations*.
- [Marcus, Marcinkiewicz, and Santorini 1993] Marcus, M. P.; Marcinkiewicz, M. A.; and Santorini, B. 1993. Building a large annotated corpus of English: The Penn Treebank. *Computational linguistics* 19(2):313–330.
- [Mori et al. 2017] Mori, H.; Youkawa, T.; Izumi, S.; Yoshimoto, M.; Kawaguchi, H.; and Inoue, A. 2017. A layer-block-wise pipeline for memory and bandwidth reduction in distributed deep learning. In *2017 IEEE 27th International Workshop on Machine Learning for Signal Processing (MLSP)*, 1–6. IEEE.
- [Renggli et al. 2018] Renggli, C.; Alistarh, D.; Hoefler, T.; and Aghagolzadeh, M. 2018. SparCML: High-performance sparse communication for machine learning. *arXiv preprint arXiv:1802.08021*.
- [Shi et al. 2019] Shi, S.; Zhao, K.; Wang, Q.; Tang, Z.; and Chu, X. 2019. A convergence analysis of distributed SGD with communication-efficient gradient sparsification. In *Proceedings of the Twenty-Eighth International Joint Conference on Artificial Intelligence, IJCAI-19*, 3411–3417.
- [Shi, Chu, and Li 2019] Shi, S.; Chu, X.; and Li, B. 2019. MG-WFBP: Efficient data communication for distributed synchronous SGD algorithms. In *INFOCOM 2019-IEEE Conference on Computer Communications, IEEE*.
- [Simonyan and Zisserman 2014] Simonyan, K., and Zisserman, A. 2014. Very deep convolutional networks for large-scale image recognition. *arXiv preprint arXiv:1409.1556*.
- [Stich, Cordonnier, and Jaggi 2018] Stich, S. U.; Cordonnier, J.-B.; and Jaggi, M. 2018. Sparsified SGD with memory. In

Advances in Neural Information Processing Systems, 4452–4463.

- [Szegedy et al. 2017] Szegedy, C.; Ioffe, S.; Vanhoucke, V.; and Alemi, A. A. 2017. Inception-v4, inception-resnet and the impact of residual connections on learning. In *Thirty-First AAAI Conference on Artificial Intelligence*.
- [Wang, Pi, and Zhou 2019] Wang, S.; Pi, A.; and Zhou, X. 2019. Scalable distributed dl training: Batching communication and computation. In *Proc. of AAAI*.
- [Wangni et al. 2018] Wangni, J.; Wang, J.; Liu, J.; and Zhang, T. 2018. Gradient sparsification for communication-efficient distributed optimization. In *Advances in Neural Information Processing Systems*, 1306–1316.
- [Wen et al. 2017] Wen, W.; Xu, C.; Yan, F.; Wu, C.; Wang, Y.; Chen, Y.; and Li, H. 2017. Terngrad: Ternary gradients to reduce communication in distributed deep learning. In *Advances in neural information processing systems*, 1509–1519.
- [Wu et al. 2018] Wu, J.; Huang, W.; Huang, J.; and Zhang, T. 2018. Error compensated quantized SGD and its applications to large-scale distributed optimization. *International Conference on Machine Learning*.
- [You, Buluç, and Demmel 2017] You, Y.; Buluç, A.; and Demmel, J. 2017. Scaling deep learning on GPU and knights landing clusters. In *Proceedings of the International Conference for High Performance Computing, Networking, Storage and Analysis*, 9. ACM.
- [Zhang et al. 2017] Zhang, H.; Zheng, Z.; Xu, S.; Dai, W.; Ho, Q.; Liang, X.; Hu, Z.; Wei, J.; Xie, P.; and Xing, E. P. 2017. Poseidon: An efficient communication architecture for distributed deep learning on GPU clusters. In *2017 USENIX Annual Technical Conference (USENIX ATC 17)*, 181–193.
- [Zheng, Huang, and Kwok 2019] Zheng, S.; Huang, Z.; and Kwok, J. T. 2019. Communication-efficient distributed block-wise momentum sgd with error-feedback. *arXiv preprint arXiv:1905.10936*.
- [Zinkevich et al. 2010] Zinkevich, M.; Weimer, M.; Li, L.; and Smola, A. J. 2010. Parallelized stochastic gradient descent. In *Advances in neural information processing systems*, 2595–2603.

A Supplementary Material

Proof of Corollary 1

Proof. For ease of presentation, we use the following abbreviations:

$$G(\mathbf{v}_t) = \frac{1}{P} \sum_{p=1}^P G^p(\mathbf{v}_t), \quad (21)$$

$$\mathbf{g}_t = \sum_{p=1}^P (\alpha_t G^p(\mathbf{v}_t) + \boldsymbol{\epsilon}_t^p), \quad (22)$$

and

$$\mathbf{g}_t^{(l)} = \sum_{p=1}^P (\alpha_t G^p(\mathbf{v}_t)^{(l)} + \boldsymbol{\epsilon}_t^{p,(l)}), \text{ for } l = 1, 2, \dots, L. \quad (23)$$

We have $\mathbf{g}_t = \sqcup_{l=1}^L \mathbf{g}_t^{(l)}$ and $\boldsymbol{\epsilon}_t = \mathbf{g}_t - \sum_{p=1}^P \alpha_t G^p(\mathbf{v}_t)^{(l)}$. According to the update formulas of \mathbf{v}_{t+1} and \mathbf{x}_{t+1} , we have

$$\begin{aligned} & \|\mathbf{v}_{t+1} - \mathbf{x}_{t+1}\|^2 \\ &= \|\mathbf{v}_t - \frac{1}{P} \sqcup_{l=1}^L \sum_{p=1}^P \text{TopK}(\alpha_t G^p(\mathbf{v}_t)^{(l)} + \boldsymbol{\epsilon}_t^{p,(l)}, k^{(l)}) \\ & \quad - (\mathbf{x}_t - \frac{1}{P} \sqcup_{l=1}^L \sum_{p=1}^P \alpha_t G^p(\mathbf{v}_t)^{(l)})\|^2 \\ &= \|\sqcup_{l=1}^L (\mathbf{v}_t^{(l)} - \frac{1}{P} \sum_{p=1}^P \text{TopK}(\mathbf{g}^{p,(l)}, k^{(l)})) \\ & \quad - \sqcup_{l=1}^L (\mathbf{x}_t^{(l)} - \frac{1}{P} \sum_{p=1}^P \alpha_t G^p(\mathbf{v}_t)^{(l)})\|^2 \\ &= \|\sqcup_{l=1}^L (\mathbf{v}_t^{(l)} - \frac{1}{P} \sum_{p=1}^P \text{TopK}(\mathbf{g}^{p,(l)}, k^{(l)}) \\ & \quad - \mathbf{x}_t^{(l)} + \frac{1}{P} \sum_{p=1}^P \alpha_t G^p(\mathbf{v}_t)^{(l)})\|^2 \\ &= \sum_{l=1}^L \|\mathbf{v}_t^{(l)} - \frac{1}{P} \sum_{p=1}^P \text{TopK}(\mathbf{g}^{p,(l)}, k^{(l)}) \\ & \quad - \mathbf{x}_t^{(l)} + \frac{1}{P} \sum_{p=1}^P \alpha_t G^p(\mathbf{v}_t)^{(l)}\|^2 \\ &= \sum_{l=1}^L \left\| -\frac{1}{P} \sum_{p=1}^P \text{TopK}(\mathbf{g}^{p,(l)}, k^{(l)}) \right. \\ & \quad \left. + \frac{1}{P} \sum_{p=1}^P \boldsymbol{\epsilon}_t^{p,(l)} + \frac{1}{P} \sum_{p=1}^P \alpha_t G^p(\mathbf{v}_t)^{(l)} \right\|^2 \end{aligned}$$

$$\begin{aligned} &= \sum_{l=1}^L \left\| \frac{1}{P} \sum_{p=1}^P \mathbf{g}_t^{p,(l)} - \frac{1}{P} \sum_{p=1}^P \text{TopK}(\mathbf{g}^{p,(l)}, k^{(l)}) \right\|^2 \\ &= \left\| \sqcup_{l=1}^L \left(\frac{1}{P} \sum_{p=1}^P \mathbf{g}_t^{p,(l)} - \frac{1}{P} \sum_{p=1}^P \text{TopK}(\mathbf{g}^{p,(l)}, k^{(l)}) \right) \right\|^2 \\ &= \left\| \frac{1}{P} \sum_{p=1}^P \mathbf{g}_t^p - \frac{1}{P} \sqcup_{l=1}^L \left(\sum_{p=1}^P \text{TopK}(\mathbf{g}^{p,(l)}, k^{(l)}) \right) \right\|^2. \end{aligned}$$

Applying Lemma 1, we have

$$\begin{aligned} & \|\mathbf{v}_{t+1} - \mathbf{x}_{t+1}\|^2 \\ &= \left\| \frac{1}{P} \sum_{p=1}^P \mathbf{g}_t^p - \frac{1}{P} \sqcup_{l=1}^L \left(\sum_{p=1}^P \text{TopK}(\mathbf{g}^{p,(l)}, k^{(l)}) \right) \right\|^2 \\ &\leq (1 - \frac{1}{c_{max}}) \left\| \frac{1}{P} \sum_{p=1}^P \mathbf{g}_t^p \right\|^2 = (1 - \frac{1}{c_{max}}) \|\alpha_t G(\mathbf{v}_t) + \mathbf{v}_t - \mathbf{x}_t\|^2 \\ &\leq (1 - \frac{1}{c_{max}}) \left((1 + \eta) \|\alpha_t G(\mathbf{v}_t)\|^2 + (1 + \frac{1}{\eta}) \|\mathbf{v}_t - \mathbf{x}_t\|^2 \right), \end{aligned}$$

where $\eta > 0$. Iterating the above inequality from $i = 0 \rightarrow t$ yields:

$$\begin{aligned} & \|\mathbf{v}_t - \mathbf{x}_t\|^2 \\ &\leq (1 - \frac{1}{c_{max}}) (1 + \frac{1}{\eta}) \sum_{i=1}^t \left((1 - \frac{1}{c_{max}}) (1 + \eta) \right)^{i-1} \|\alpha_{t-i} G(\mathbf{v}_{t-i})\|^2 \\ &= \frac{1}{\eta} \sum_{i=1}^t \left((1 - \frac{1}{c_{max}}) (1 + \eta) \right)^i \|\alpha_{t-i} G(\mathbf{v}_{t-i})\|^2 \end{aligned}$$

Taking the expectation and using the bound of the second moment on stochastic gradients: $\mathbb{E}[\|G(\mathbf{v}_t)\|^2] \leq M^2$, we obtain

$$\begin{aligned} & \mathbb{E} [\|\mathbf{v}_t - \mathbf{x}_t\|^2] \\ &\leq \frac{1}{\eta} \sum_{i=1}^t \left((1 - \frac{1}{c_{max}}) (1 + \eta) \right)^i \mathbb{E} [\|\alpha_{t-i} G(\mathbf{v}_{t-i})\|^2] \\ &\leq \frac{1}{\eta} \sum_{i=1}^t \left((1 - \frac{1}{c_{max}}) (1 + \eta) \right)^i \alpha_{t-i}^2 M^2, \end{aligned}$$

which concludes the proof. \square

Proof of Theorem 1

Proof. We use the Lipschitz continuity property of f and Corollary 1 to derive the bound of (14). First, with the Lipschitz constant C of f , we have

$$\begin{aligned} f(\mathbf{x}_{t+1}) - f(\mathbf{x}_t) &\leq \nabla f(\mathbf{x}_t)^T (\mathbf{x}_{t+1} - \mathbf{x}_t) + \frac{C}{2} \|\mathbf{x}_{t+1} - \mathbf{x}_t\|^2 \\ &= \alpha_t \nabla f(\mathbf{x}_t)^T G(\mathbf{v}_t) + \frac{\alpha_t^2 C}{2} \|G(\mathbf{v}_t)\|^2. \end{aligned}$$

Taking the expectation with respect to sampling at iteration t , it yields

$$\begin{aligned}
& \mathbb{E}_t[f(\mathbf{x}_{t+1})] - f(\mathbf{x}_t) \\
& \leq \alpha_t \nabla f(\mathbf{x}_t)^T \mathbb{E}_t[G(\mathbf{v}_t)] + \frac{\alpha_t^2 C}{2} \mathbb{E}_t[\|G(\mathbf{v}_t)\|^2] \\
& = \alpha_t \nabla f(\mathbf{x}_t)^T \nabla f(\mathbf{v}_t) + \frac{\alpha_t^2 C}{2} \mathbb{E}_t[\|G(\mathbf{v}_t)\|^2] \\
& = -\frac{\alpha_t}{2} \|\nabla f(\mathbf{x}_t)\|^2 - \frac{\alpha_t}{2} \|\nabla f(\mathbf{v}_t)\|^2 \\
& \quad + \frac{\alpha_t}{2} \|\nabla f(\mathbf{x}_t) - \nabla f(\mathbf{v}_t)\|^2 + \frac{\alpha_t^2 C}{2} \mathbb{E}_t[\|G(\mathbf{v}_t)\|^2] \\
& \leq -\frac{\alpha_t}{2} \|\nabla f(\mathbf{x}_t)\|^2 + \frac{\alpha_t C^2}{2} \|\mathbf{v}_t - \mathbf{x}_t\|^2 + \frac{\alpha_t^2 C M^2}{2} \\
& = -\frac{\alpha_t}{2} (\|\nabla f(\mathbf{x}_t)\|^2 + C^2 \|\mathbf{v}_t - \mathbf{x}_t\|^2) \\
& \quad + \alpha_t C^2 \|\mathbf{v}_t - \mathbf{x}_t\|^2 + \frac{\alpha_t^2 C M^2}{2}.
\end{aligned}$$

Taking the expectation with respect to the gradients before iteration t , it yields

$$\begin{aligned}
& \mathbb{E}[f(\mathbf{x}_{t+1})] - \mathbb{E}[f(\mathbf{x}_t)] \\
& \leq -\frac{\alpha_t}{2} \mathbb{E}[\|\nabla f(\mathbf{x}_t)\|^2 + C^2 \|\mathbf{v}_t - \mathbf{x}_t\|^2] \\
& \quad + \alpha_t C^2 \mathbb{E}[\|\mathbf{v}_t - \mathbf{x}_t\|^2] + \frac{\alpha_t^2 C M^2}{2}.
\end{aligned}$$

Using Corollary 1, we obtain

$$\begin{aligned}
& \mathbb{E}[f(\mathbf{x}_{t+1})] - \mathbb{E}[f(\mathbf{x}_t)] \\
& \leq \frac{\alpha_t C^2}{\eta} \sum_{i=1}^t \left(\left(1 - \frac{1}{c_{max}}\right) (1 + \eta) \right)^i \alpha_{t-i}^2 M^2 + \frac{\alpha_t^2 C M^2}{2} \\
& \quad - \frac{\alpha_t}{2} \mathbb{E}[\|\nabla f(\mathbf{x}_t)\|^2 + C^2 \|\mathbf{v}_t - \mathbf{x}_t\|^2] \\
& = \frac{\alpha_t^2 C^2}{\eta} \sum_{i=1}^t \left(\left(1 - \frac{1}{c_{max}}\right) (1 + \eta) \right)^i \frac{\alpha_{t-i}^2}{\alpha_t} M^2 + \frac{\alpha_t^2 C M^2}{2} \\
& \quad - \frac{\alpha_t}{2} \mathbb{E}[\|\nabla f(\mathbf{x}_t)\|^2 + C^2 \|\mathbf{v}_t - \mathbf{x}_t\|^2].
\end{aligned}$$

If (15) holds, then we have

$$\begin{aligned}
& \mathbb{E}[f(\mathbf{x}_{t+1})] - \mathbb{E}[f(\mathbf{x}_t)] \\
& \leq \left(C + \frac{2C^2 D}{\eta} \right) \frac{M^2 \alpha_t^2}{2} - \frac{\alpha_t}{2} \mathbb{E}[\|\nabla f(\mathbf{x}_t)\|^2 + C^2 \|\mathbf{v}_t - \mathbf{x}_t\|^2].
\end{aligned}$$

Adjusting the order, we obtain

$$\begin{aligned}
& \alpha_t \mathbb{E}[\|\nabla f(\mathbf{x}_t)\|^2 + C^2 \|\mathbf{v}_t - \mathbf{x}_t\|^2] \\
& \leq 2(\mathbb{E}[f(\mathbf{x}_t)] - \mathbb{E}[f(\mathbf{x}_{t+1})]) + \left(C + \frac{2C^2 D}{\eta} \right) M^2 \alpha_t^2. \quad (24)
\end{aligned}$$

We further apply the property of f , that is

$$\begin{aligned}
\|\nabla f(\mathbf{v}_t)\|^2 & = \|\nabla f(\mathbf{v}_t) - \nabla f(\mathbf{x}_t) + \nabla f(\mathbf{x}_t)\|^2 \\
& \leq 2\|\nabla f(\mathbf{v}_t) - \nabla f(\mathbf{x}_t)\|^2 + 2\|\nabla f(\mathbf{x}_t)\|^2 \\
& \leq 2C^2 \|\mathbf{v}_t - \mathbf{x}_t\|^2 + 2\|\nabla f(\mathbf{x}_t)\|^2.
\end{aligned}$$

Together with (24), it yields

$$\begin{aligned}
& \alpha_t \mathbb{E}[\|\nabla f(\mathbf{v}_t)\|^2] \\
& \leq 2\alpha_t \mathbb{E}[C^2 \|\mathbf{v}_t - \mathbf{x}_t\|^2 + \|\nabla f(\mathbf{x}_t)\|^2] \\
& \leq 4(\mathbb{E}[f(\mathbf{x}_t)] - \mathbb{E}[f(\mathbf{x}_{t+1})]) + 2\left(C + \frac{2C^2 D}{\eta}\right) M^2 \alpha_t^2.
\end{aligned}$$

Summing up the inequality for $t = 1, 2, \dots, T$, it yields

$$\begin{aligned}
& \sum_{t=1}^T \alpha_t \mathbb{E}[\|\nabla f(\mathbf{v}_t)\|^2] \\
& \leq 4(f(\mathbf{x}_0) - f(\mathbf{x}^*)) + 2\left(C + \frac{2C^2 D}{\eta}\right) M^2 \sum_{t=1}^T \alpha_t^2.
\end{aligned}$$

Multiplying $\frac{1}{\sum_{t=1}^T \alpha_t}$ in both sides, it yields

$$\begin{aligned}
& \frac{1}{\sum_{t=1}^T \alpha_t} \sum_{t=1}^T \alpha_t \mathbb{E}[\|\nabla f(\mathbf{v}_t)\|^2] \\
& \leq \frac{4(f(\mathbf{x}_0) - f(\mathbf{x}^*))}{\sum_{t=1}^T \alpha_t} + \frac{2\left(C + \frac{2C^2 D}{\eta}\right) M^2 \sum_{t=1}^T \alpha_t^2}{\sum_{t=1}^T \alpha_t},
\end{aligned}$$

which concludes the proof. \square

Proof of Corollary 2

Proof. As $\alpha_t = \theta/\sqrt{T}$, we simplify the notations by: $\alpha = \alpha_t = \theta/\sqrt{T}$ and $\tau = (1 - \frac{1}{c_{max}})(1 + \eta)$. Then the left hand side of (15) becomes

$$\begin{aligned}
& \sum_{i=1}^t \left(\left(1 - \frac{1}{c_{max}}\right) (1 + \eta) \right)^i \frac{\alpha_{t-i}^2}{\alpha_t} \\
& = \sum_{i=1}^t \tau^i \frac{\alpha_{t-i}^2}{\alpha_t} = \alpha \sum_{i=1}^t \tau^i \\
& = \alpha \frac{\tau(1 - \tau^t)}{1 - \tau}.
\end{aligned}$$

Choosing $\eta = \frac{1}{c_{max}}$ to make $0 \leq \tau = (1 - \frac{1}{c_{max}})(1 + \eta) < 1$ hold, we have

$$\lim_{t \rightarrow \infty} \alpha \frac{\tau(1 - \tau^t)}{1 - \tau} = \frac{\alpha \tau}{1 - \tau}.$$

Then inequality (15) holds when $D = \frac{\alpha \tau}{1 - \tau}$. By applying Theorem 1, we obtain

$$\begin{aligned}
& \mathbb{E} \left[\frac{1}{T} \sum_{t=1}^T \|\nabla f(\mathbf{v}_t)\|^2 \right] \\
& \leq \frac{4(f(\mathbf{x}_0) - f(\mathbf{x}^*))}{\alpha T} + 2\left(C + \frac{2C^2 D}{\eta}\right) M^2 \alpha \\
& = \frac{4\theta^{-1}(f(\mathbf{x}_0) - f(\mathbf{x}^*))}{\sqrt{T}} + \frac{2CM^2\theta}{\sqrt{T}} + \frac{4\frac{\tau}{(1-\tau)\eta}C^2M^2\theta^2}{T} \\
& = \frac{4\theta^{-1}(f(\mathbf{x}_0) - f(\mathbf{x}^*)) + 2\theta CM^2}{\sqrt{T}} + \frac{4C^2M^2(c_{max}^3 - c_{max})\theta^2}{T},
\end{aligned}$$

which concludes the proof. \square